

Supporting Information

1. Experimental section

1.1 Materials syntheses

Sulfonated Zirconium-based MOF: In a process, 0.233 g of $ZrCl_4$ and 0.332 g of terephthalic acid were added to 32 mL of N, N-dimethylformamide (DMF). To this solution, 4 mL of concentrated HCl and 4 mL of acetic acid were added, and the mixture was vigorously stirred until the solution became clear. Separately, 0 g, 0.01 g, 0.03 g, and 0.05 g of polystyrene sulfonic acid (PSS) were added to 5 mL of deionized water, and each solution was stirred until it became clear. Subsequently, solutions of different PSS concentrations were dropwise added to four portions of the previously prepared DMF solution. After thorough mixing, the reaction mixtures were stirred at 80°C in a water bath for 24 hours. Upon completion of the reaction, the resulting materials (designated as MOF-PSS(0), MOF-PSS(1), MOF-PSS(3), and MOF-PSS(5)) were washed by repeated exchanges with DMF and deionized water six times and then dried at 60°C to obtain white powders.^{1,2,3}

Sulfonated/Un sulfonated QSSE: Initially, 3.6563 g of $Zn(CF_3SO_3)_2$ was individually dissolved in five portions of 10 mL deionized water to create five 1 mol L⁻¹ $Zn(CF_3SO_3)_2$ aqueous solutions. Among these, one solution remained without MOF, while the other four solutions incorporated 0.03 g of MOF with varying degrees of sulfonation. Ultrasonication was applied until no visible powder particles were observed, followed by thorough stirring for 2 hours. Subsequently, 3 g of PVA was slowly added to each of the five mixed solutions under gentle stirring. Afterward, the mixture was stirred at room temperature for 30 minutes. Then, the temperature was gradually raised from room temperature to 90°C while maintaining stirring. The temperature was held at 90°C until the complete dissolution of PVA, which took approximately 4 hours. The prepared precursor solution was poured into a suitable container while hot, adjusted to achieve the desired film thickness, and allowed to rest to eliminate air bubbles. Subsequently, the container with the precursor solution was transferred to a -24°C freezer, where it was frozen for 6 hours. Finally, the QSSE membrane was obtained through natural thawing. The resulting QSSE is self-supporting with a certain degree of viscosity, making it suitable for direct use as a separator.^{4,5}

Polyaniline/Carbon Cloth (PANI/CC): Initially, a 3×3 cm² carbon cloth was immersed in a 90 mL 1 mol L⁻¹ H_2SO_4 solution. Afterward, 1 g of polyvinylpyrrolidone (PVP) was added, and the mixture was stirred for 1 hour to facilitate hydrophilic treatment. Next, the system was transferred to an ice bath, and 0.6975 mL of aniline was added, followed by stirring for 30 minutes. Subsequently, a 10 mL 1 mol L⁻¹ H_2SO_4 solution containing 1.71 g of ammonium persulfate [$(NH_4)_2S_2O_8$] was slowly added drop by drop to the system, preferably completing the addition within 10 minutes. After stirring in the ice bath for 1 hour, the reaction mixture was transferred to a 0°C refrigerator and allowed to continue reacting for 23 hours. Upon completion of the reaction, the carbon

cloth was removed, washed with deionized water and ethanol until the wash solution became colorless, and finally, it was dried at 60°C to obtain carbon cloth with a black-green surface. This material was then cut into 8 mm diameter circular pieces for later use.⁶

1.2 Characterization

XRD testing was conducted using the Bruker AXS D8 Advance X-ray diffractometer to perform phase identification and structural analysis of the materials. The FT-IR testing was conducted using the Nicolet 6700 instrument, which has the following main performance parameters. Infrared spectral range: 4000~50 cm⁻¹; Spectral resolution: Better than 0.09 cm⁻¹; Wavenumber accuracy: 0.005 cm⁻¹; Signal-to-noise ratio: Better than 13,000:1 (5 seconds); Interferometer: Possesses ultra-high stability with position accuracy of ±0.2 nm, ensuring long-term detection stability, accuracy, and preventing spectral deviation and distortion; Detector: Equipped with three detectors, including the mid-infrared DLaTGS detector, enhanced DTGS detector, and liquid nitrogen-cooled MCT-A detector. The SEM testing was performed using the Hitachi SU8010 instrument from Japan, which has the following main technical specifications. Accelerating Voltage: 0.1~30 kV; Magnification Range: 20~1,200,000x; Secondary Electron Resolution: 1.0 nm (at 15 kV), 1.3 nm (at 1 kV); Working Distance: 0.5~30 mm.

1.3 Electrochemical measurements

The electrochemical tests were conducted using CR2016 button cells. For the Zn||SS cell assembly: The cell utilizes a zinc electrode as the working electrode and a stainless steel sheet as the counter electrode. For the Zn||Zn cell assembly: In this cell, both zinc electrodes serve as the working electrodes, and a quasi-solid-state electrolyte is used as the separator. During the cell assembly, efforts should be made to align the two zinc electrode pieces completely and form concentric circles with the separator. For the assembly of the full cell: The full cell assembly involves using the prepared PANI/CC positive electrode and zinc foil as the working electrodes, with the prepared QSSE serving as both the separator and electrolyte. All of the aforementioned batteries were assembled in the presence of atmospheric air.

2. Property Characterizations

The ionic conductivity was measured by assembling stainless steel (SS)//electrolyte//SS CR2016 cells using alternating-current (AC) impedance spectra at the temperatures of 25°C by electrochemical workstation (CHI 760E) in the frequency range from 0.01 MHz to 100 KHz (AC amplitude = 5mV). The ionic conductivity (σ) was calculated based on the following equation:

$$\sigma = \frac{L}{RA} \quad (1)$$

where L represents the thickness of the electrolyte membrane, R is the bulk resistance of electrolytes, and A refers to the contact area between electrolytes and SS electrodes (16 mm).⁷

The zinc ion transference number (t_+) was tested in Zn//electrolyte//Zn cells at 25 °C and calculated according to following formula:

$$t_+ = \frac{I_{(t=\infty)}(\Delta V - I_{(t=0)}R_{(t=0)})}{I_{(t=0)}(\Delta V - I_{(t=\infty)}R_{(t=\infty)})} \quad (2)$$

where ΔV is the applied direct-current (DC) polarization voltage (10 mV), $I_{(t=0)}$ and $R_{(t=0)}$ are the initial current and resistance value before polarization, $I_{(t=\infty)}$ and $R_{(t=\infty)}$ are the steady current and resistance after polarization (3600 s).⁸

Zn plating/stripping cycles were conducted on symmetric Zn//electrolyte//Zn cells using LAND CT3001A charge/discharge equipment with 1mV s^{-1} from the range of -0.2 to 0.3V. The diffusion coefficients (D) are calculated by the following formula:

$$D = \frac{4}{\pi\tau} \left(\frac{m_B V_M}{M_B S} \right)^2 \left(\frac{\Delta E_S}{\Delta E_\tau} \right)^2 \quad (3)$$

where τ is the relaxation time, m_B is the number of moles of electrons transferred by lithium metal, V_M is the molar volume of the electrode material, which can be calculated by measuring the density, S is the contact area between electrode and electrolyte, ΔE_S is the voltage change induced by the pulse, ΔE_τ is the galvanostatic charge (discharge) voltage change.⁹ The activation energy (E_a) is calculated by the following formula:

$$\sigma = A \exp\left(\frac{-E_a}{RT}\right) \quad (4)$$

where σ is the ionic conductivity at different temperatures, E_a is the activation energy, T is the absolute temperature, and A is the pre-exponential factor.¹⁰

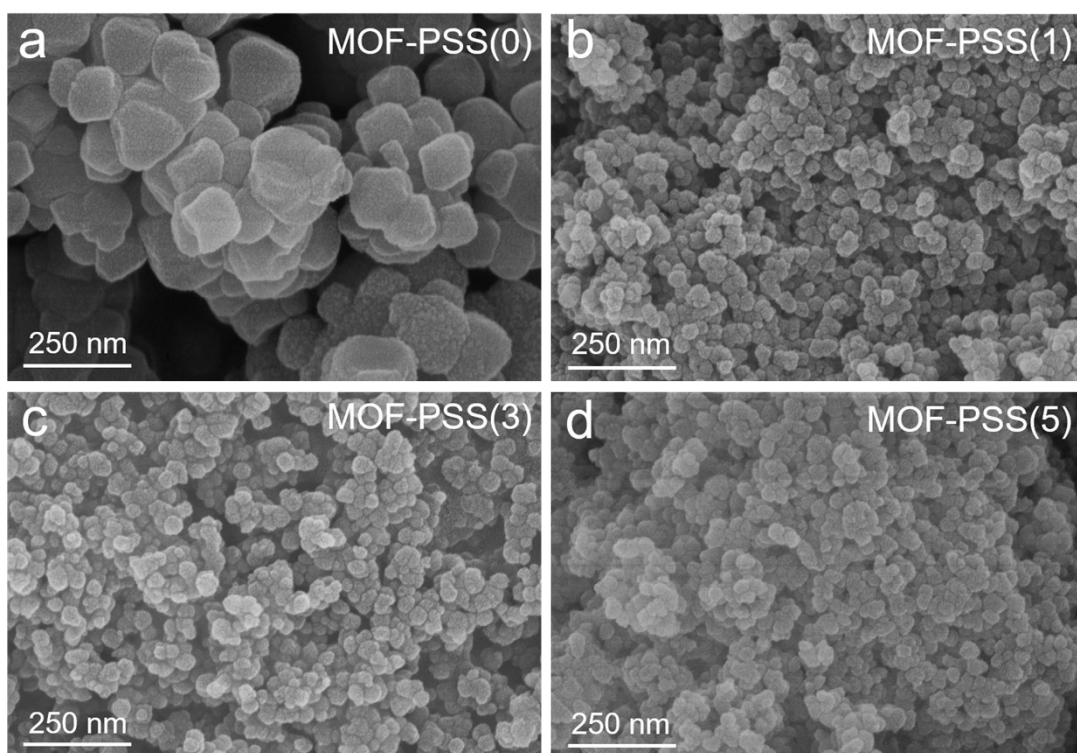


Figure S1: These modifiers were denoted as MOF-PSS(0), MOF-PSS(1), MOF-PSS(3), and MOF-PSS(5) depending on the varying concentrations of the PSS water solution added during synthesis. SEM characterization of MOFs with different sulfonation degrees, depicting (a) MOF-PSS(0); (b) MOF-PSS(1); (c) MOF-PSS(3), and (d) MOF-PSS(5).

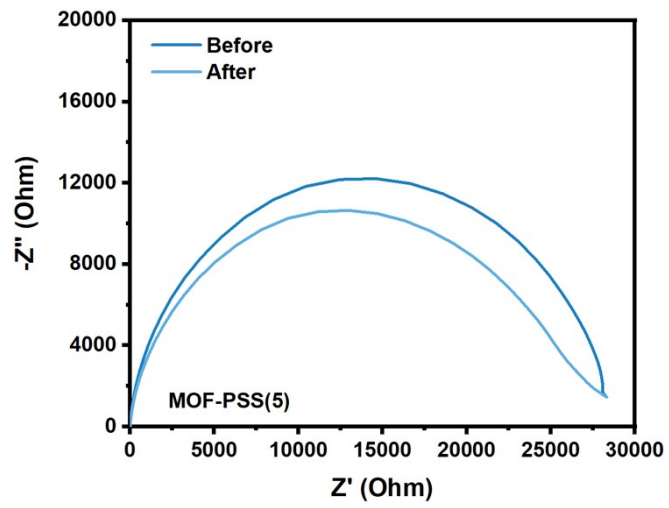


Figure S2: Impedance diagram of MOF-PSS(5)-Modified QSSE before and after potentiostatic polarization testing.

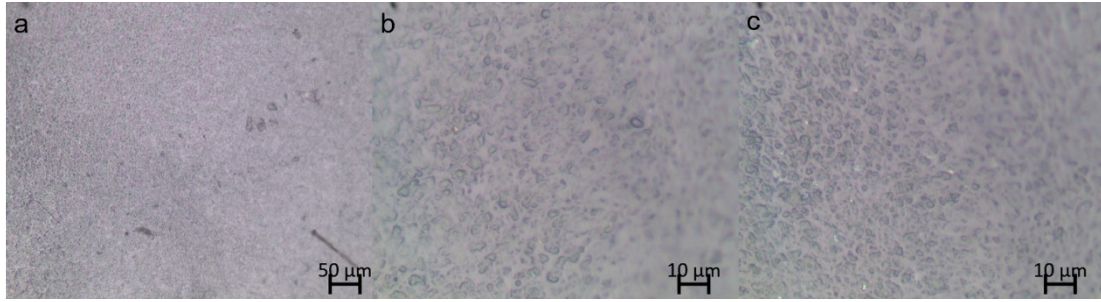


Figure S3: QSSE surface after 10 hours lyophilization treatment at -80°C under (a)10x;(b) and (c)50x microscope.

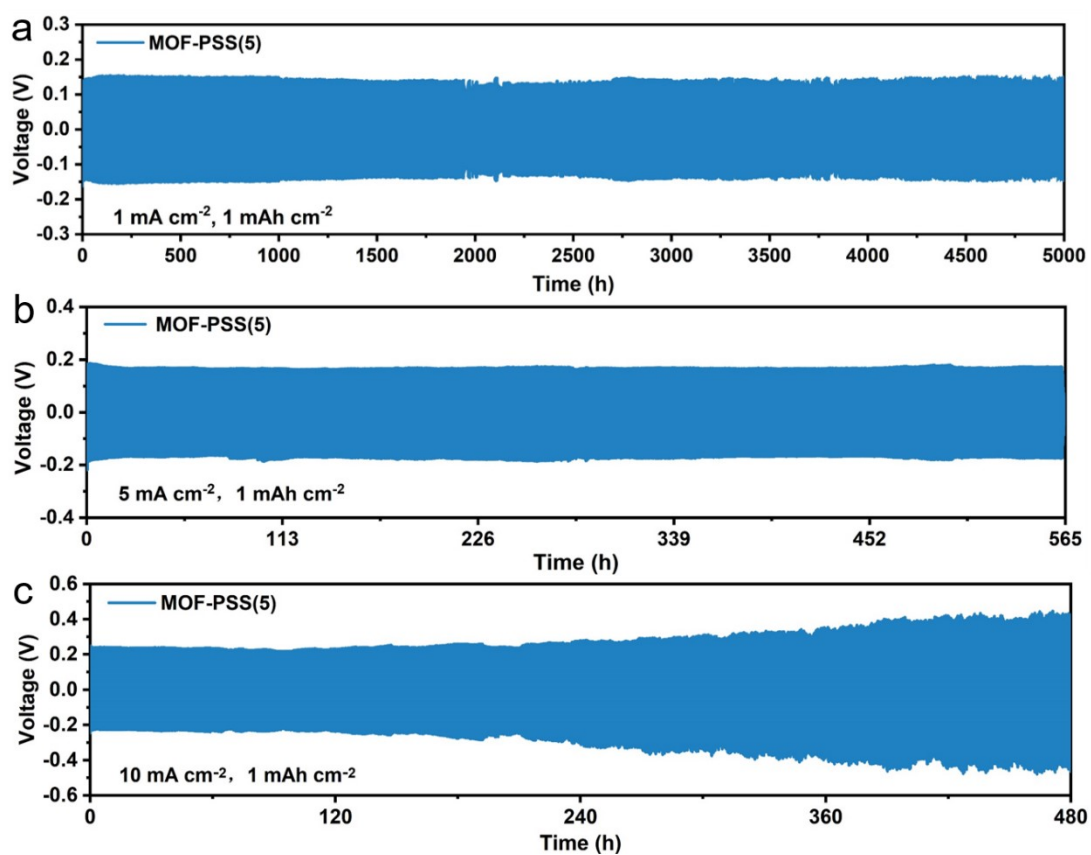


Figure S4: Long cycling performance of MOF-PSS(5)-Modified QSSE at (a) 10 mA cm^{-2} , 1 mAh cm^{-2} ; (b) 5 mA cm^{-2} , 1 mAh cm^{-2} , and (c) 1 mA cm^{-2} , 1 mAh cm^{-2} .

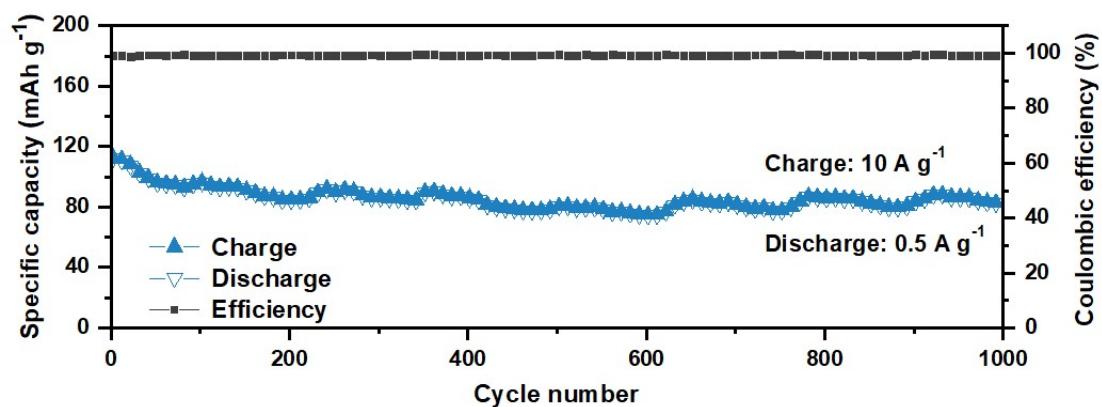


Figure S5: The long cycling performance of a full cell using MOF-PSS(5)-modified QSSE under simulated fast-charging and slow-discharging conditions was evaluated.

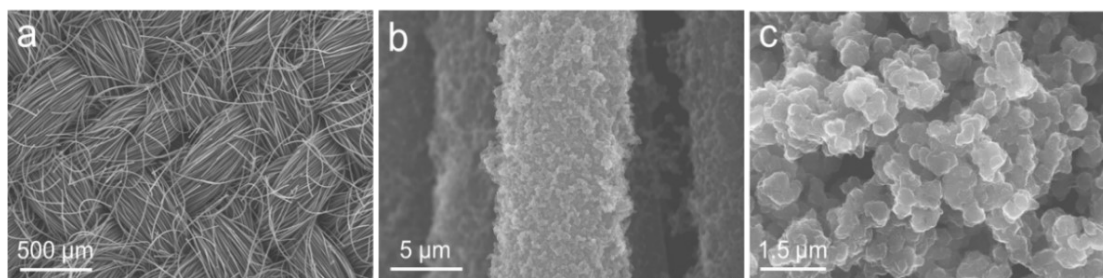


Figure S6: SEM characterizations of PANI/CC: (a)500 μm ; (b)5 μm ; (c)1.5 μm ;

To implement the prepared QSSE in ZIBs, a positive electrode material, polyaniline/carbon cloth (PANI/CC), suitable for QSSZIBs was prepared. The SEM characterization of PANI/CC is illustrated in **Figure. S6a-c**. At low magnification, the carbon cloth substrate can be observed, consisting of carbon fibers bundled and interwoven. Polyaniline, synthesized in situ, forms continuous nanoparticles (with a diameter of approximately 50 nm) that uniformly envelop the carbon fibers.

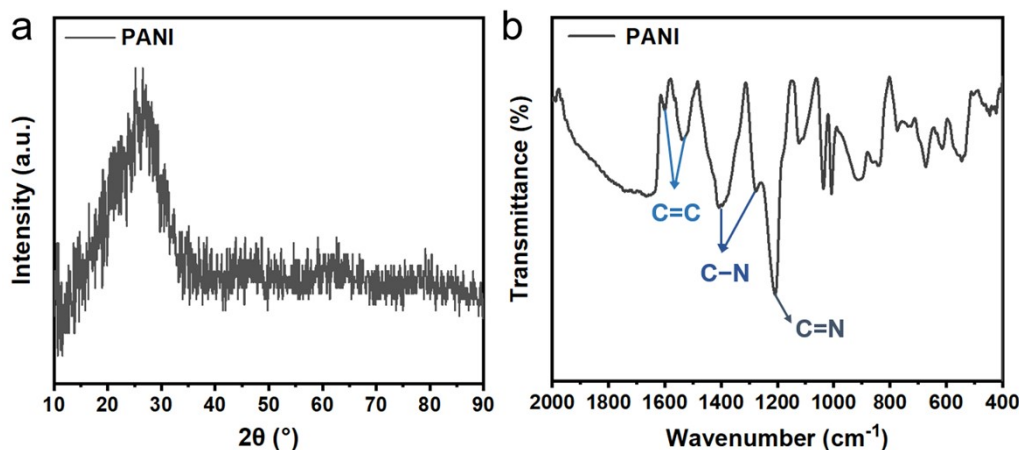


Figure S7: (a) XRD and (b) FT-IR characterization of PANI in the reaction system;

As for the XRD characterization shown in **Figure. S7a**, the PANI synthesized through this method exhibits a typical amorphous nature. A broad diffraction peak at around 27° is observed, attributed to the scattering of PANI molecular chains. The molecular structure of PANI is validated through FT-IR characterization, as seen in **Figure. S7b**. There are two peaks around 1600 cm^{-1} and 1536 cm^{-1} , arising from stretching vibrations of the quinoid structure and the C=C bonds in the benzene ring.¹¹ Peaks at 1397 cm^{-1} and 1275 cm^{-1} are attributed to the absorption of the C-N structure in the aromatic amine, while the peak at 1211 cm^{-1} corresponds to the stretching vibration of the C=N group in the quinone ring. The presence of these characteristic peaks confirms the formation of emeraldine structure in PANI.¹²

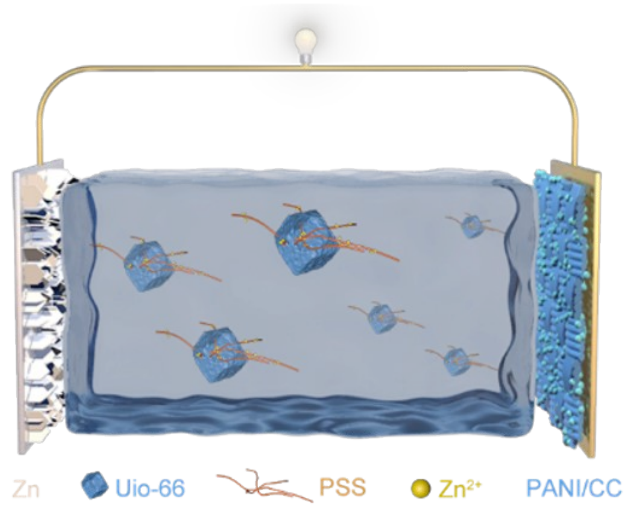


Figure S8: Illustration of a full cell with zinc foil as the negative electrode and PANI/CC as the positive electrode.

Table S1: Parameters for ion conductivity measurements of QSSE with various fillers.

Fillers	Thickness(mm)	Diameter(mm)
Without MOF	1.0	15
MOF-PSS(0)	1.5	15
MOF-PSS(1)	1.0	11
MOF-PSS(3)	2.0	11
MOF-PSS(5)	1.5	11

- (1) Li, R.; Jiang, J.; Liu, Q.; Xie, Z.; Zhai, J. Hybrid Nanochannel Membrane Based on Polymer/MOF for High-Performance Salinity Gradient Power Generation. *Nano Energy* **2018**, *53*, 643–649.
- (2) Ma, X.; Fang, W.; Guo, Y.; Li, Z.; Chen, D.; Ying, W.; Xu, Z.; Gao, C.; Peng, X. Hierarchical Porous SWCNT Stringed Carbon Polyhedrons and PSS Threaded MOF Bilayer Membrane for Efficient Solar Vapor Generation. *Small* **2019**, *15* (15), 1900354.
- (3) Garg, G.; Garg, N.; Deep, A.; Soni, D. Zr-MOF and PEDOT: PSS Composite Sensor for Chemoresistive Sensing of Toluene at Room Temperature. *Journal of Alloys and Compounds* **2023**, *956*, 170309.
- (4) Amaral, M. M.; Venancio, R.; Peterlevitz, A. C.; Zanin, H. Recent Advances on Quasi-Solid-State Electrolytes for Supercapacitors. *Journal of Energy Chemistry* **2022**, *67*, 697–717.
- (5) Huang, W.-H.; Li, X.-M.; Yang, X.-F.; Zhang, X.-X.; Wang, H.-H.; Wang, H. The Recent Progress and Perspectives on Metal-and Covalent-Organic Framework Based Solid-State Electrolytes for Lithium-Ion Batteries. *Materials Chemistry Frontiers* **2021**, *5* (9), 3593–3613.
- (6) Ahirrao, D. J.; Pal, A. K.; Singh, V.; Jha, N. Nanostructured Porous Polyaniline (PANI) Coated Carbon Cloth (CC) as Electrodes for Flexible Supercapacitor Device. *Journal of Materials Science & Technology* **2021**, *88*, 168–182.
- (7) Qian, X.; Gu, N.; Cheng, Z.; Yang, X.; Wang, E.; Dong, S. Methods to Study the Ionic Conductivity of Polymeric Electrolytes Using Ac Impedance Spectroscopy. *Journal of Solid State Electrochemistry* **2001**, *6*, 8–15.
- (8) Zugmann, S.; Fleischmann, M.; Amereller, M.; Gschwind, R. M.; Wiemhöfer, H. D.; Gores, H. J. Measurement of Transference Numbers for Lithium Ion Electrolytes via Four Different Methods, a Comparative Study. *Electrochimica Acta* **2011**, *56* (11), 3926–3933.
- (9) Nickol, A.; Schied, T.; Heubner, C.; Schneider, M.; Michaelis, A.; Bobeth, M.; Cuniberti, G. GITT Analysis of Lithium Insertion Cathodes for Determining the Lithium Diffusion Coefficient at Low Temperature: Challenges and Pitfalls. *Journal of The Electrochemical Society* **2020**, *167* (9), 090546.
- (10) Ozawa, T. Estimation of Activation Energy by Isoconversion Methods. *Thermochimica acta* **1992**, *203*, 159–165.
- (11) Yanilmaz, M.; Dirican, M.; Asiri, A. M.; Zhang, X. Flexible Polyaniline-Carbon Nanofiber Supercapacitor Electrodes. *Journal of Energy Storage* **2019**, *24*, 100766.
- (12) Hsieh, Y.-Y.; Zhang, Y.; Zhang, L.; Fang, Y.; Kanakaraaj, S. N.; Bahk, J.-H.; Shanov, V. High Thermoelectric Power-Factor Composites Based on Flexible Three-Dimensional Graphene and Polyaniline. *Nanoscale* **2019**, *11* (14), 6552–6560.